JACS
JOURNAL OF THE AMERICAN CHEMICAL SOCIETY

Communication

Spectroscopic Evidence for Acid-Catalyzed Disproportionation Reaction of Oxoiron(IV) Porphyrin to Oxoiron(IV) Porphyrin #-Cation Radical and Iron(III) Porphyrin

Kana Nishikawa, Yuki Honda, and Hiroshi Fujii

J. Am. Chem. Soc., **Just Accepted Manuscript** • DOI: 10.1021/jacs.9b13503 • Publication Date (Web): 02 Mar 2020

Just Accepted

is published by the American Chemical Society. 1155 Sixteenth Street N.W., Washington, DC 20036

Spectroscopic Evidence for Acid-Catalyzed Disproportionation Reaction of Oxoiron(IV) Porphyrin to Oxoiron(IV) Porphyrin π-Cation Radical and Iron(III) Porphyrin

Kana Nishikawa, Yuki Honda, and Hiroshi Fujii*

Department of Chemistry, Biology, and Environmental Science, Graduate School of Humanities and Sciences, Nara Women's University, Nara 630-8506, Japan

Supporting Information Placeholder

ABSTRACT: The disproportionation reaction of oxoiron(IV) porphyrin complex (**II**) to oxoiron(IV) porphyrin π-cation radical complex (**I**) and iron(III) porphyrin complex (**III**) have been proposed in various reactions (Figure 1). However, there have been no report that clarifies the disproportionation reaction spectroscopically. Here, we show direct evidence for the disproportionation reaction of **II** with absorption, ^{2}H NMR, and EPR spectroscopy. Kinetic study of the disproportionation reaction with stopped flow technique can be analyzed as the second-order reaction for the concentration of proton and the first-order for the concentration of **II**. These results allow us to propose the mechanism of the disproportionation reaction, involving the sequential addition of two protons to the oxo ligand of **II**, to give an iron(III) porphyrin π-cation radical species, which reacts with another **II** to afford **I** and **III** (Figure 4).

High valent iron oxo species have been known as reactive intermediates in the catalytic reactions of heme and nonheme iron enzymes.[1-4] Oxoiron(IV) porphyrin π-cation radical species have been characterized in the reactions of cytochrome P450, catalases, and peroxidases, and referred to as Compound I (Comp I).[4-5] Much attention has been directed toward the reactions of Comp I because it catalyzes many chemically attractive reactions, such as C-H bond activations. The reaction of Comp I with various substrates have been studied by using heme enzymes and their model complexes.[1] On the other hand, oxoiron(IV) porphyrin species have been found in the reactions of peroxidases and referred as Compound II (Comp II).[1, 4] Oxoiron(IV) porphyrin complexes have also been synthesized with synthetic iron porphyrin complexes. Comp II usually catalyzes one-electron oxidations of phenols and amines in the reactions of peroxidases. This reactivity is in contrast to those of oxoiron(IV) species of nonheme iron enzymes and their model complexes, which catalyze various oxygenation reactions as catalyzed by Comp I.

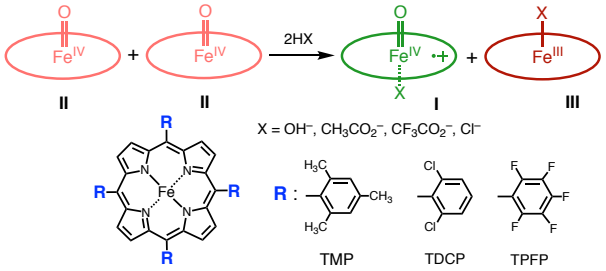

Figure 1. Disproportionation Reaction of Oxoiron(IV) porphyrin complex.

Compared with Comp I and nonheme oxoiron(IV) complexes, oxoiron(IV) porphyrin complex was initially thought to be poor oxidant that can react with only reactive substrates like triphenylphosphine.[6] Later, Groves et al. reported that oxoiron(IV) meso-tetramesitylporphyrin (**TMP-II**) is capable of epoxidation reaction.[7] Nam et al. reported that oxoiron(IV) meso-tetrakis(pentafluorophenyl)porphyrin (**TPFP-II**) is able to oxidize alkane to alcohol (eg: triphenylmethane to triphenylmethanol), as well as epoxidations of olefins, at room temperature.[8] Newcomb et al. also reported that oxoiron(IV) meso-tetrakis(2,6-dichlorophenyl)porphyrin (**TDCP-II**) and **TPFP-II** oxidize olefins, but **TDCP-II** is more reactive than **TPFP-II**.[9] The reactivity of oxoiron(IV) porphyrin complex has been reported to be unique and different from the reactivity of oxoiron(IV) π-cation radical complex.[7, 9] In some studies, the unique reactivity has been explained by the disproportionation reactions of oxoiron(IV) porphyrin complexes.[9-10] Oxoiron(IV) porphyrin (**II**) disproportionates to oxoiron(IV) porphyrin π-cation radical (**I**) and iron(III) porphyrin (**III**) in the presence of water (proton) and the compound-**I** formed acts as a reactive species for oxygenation reactions (Figure 1). Similar disproportionation reactions have been also proposed in the reactions of oxomanganese(IV)

porphyrin complexes.[11-12] Although the disproportionation reaction has been proposed in many studies,[9-12] it has been never studied spectroscopically. Since the disproportionation reaction could be catalyzed by water, we expected that the disproportionation reaction can be observed when an acid is added to oxoiron(IV) porphyrin complex. Here, we show the first evidence on the disproportionation reaction of oxoiron(IV) porphyrin complex with absorption, NMR and EPR spectroscopy. Kinetic analyses of the disproportionation reactions allow us to propose a reaction mechanism involving the successive addition of two protons to the oxo ligand of oxoiron(IV) porphyrin complex, followed by the oxidation of oxoiron(IV) porphyrin complex to oxoiron(IV) porphyrin π-cation radical complex.

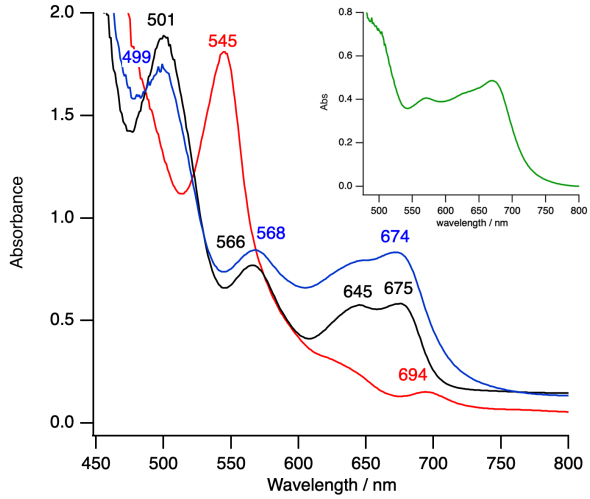

Figure 2. Absorption spectral change for the reaction of **TMP-II** with AcOH in dichloromethane at –60 °C. Red line: **TMP-II** (0.12 mM), blue line: after the addition of AcOH (0.34 mM), black line: further addition of TBAI (0.12 mM). Inset: absorption spectrum (green line) after subtraction of half intensity of the black spectrum from the blue spectrum (blue line – 0.5×black line).

TMP-II was prepared by ligand metathesis of bis-perchlorateiron(III) TMP π-cation radical over moist basic alumina at low temperature.[7] Figure 2 shows absorption spectral change for the reaction of **TMP-II** with acetic acid (AcOH, 0.34 mM) in dichloromethane at –60 °C. The absorption spectrum (red line in Figure 2) of **TMP-II** having an absorption peak at 545 nm changes to new one having absorption peaks at 499, 568, and 674 nm (blue line in Figure 2). Titration of AcOH showed that no further spectral change was observed when more than 3.0 equiv of AcOH was added and the overall spectral change consists of two steps having clear isosbestic points: 0 ~ 0.71 equiv and 0.95 ~ 3.1 equiv (Figure S1). The analysis of the first step suggests the binding of one-molecule of AcOH with the binding constant of 8×10^4 M^{-1} (Figure S2). The absorption spectral feature of the product is close to that of the 1:1 mixture of oxoiron(IV) TMP π-cation radical complex (**TMP-I**) and iron(III) TMP complex (**TMP-III**) (Figure S3). To confirm the formation of **TMP-I**, tetra-*n*-buthylammonium iodide (TBAI, 1 equiv to the initial **TMP-II**), which can reduce **TMP-I** to **TMP-III**, was added to the solution. The absorption spectrum changes to that of **TMP-III** after the addition of TBAI (black line in Figure 2). The formation of **TMP-I** is also confirmed by the difference spectrum (Inset in Figure 2). These results suggest that **TMP-II** rapidly disproportionates to **TMP-I** and **TMP-III** with the addition of AcOH.

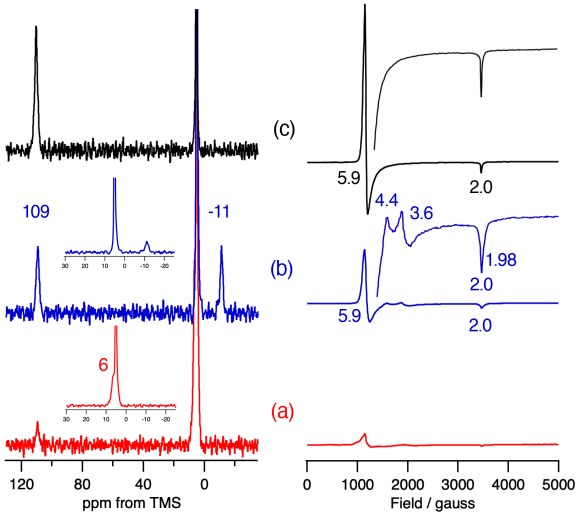

Figure 3. ^{2}H NMR (left) and EPR (right) spectral changes for the reaction of **TMP-II** with AcOH in dichloromethane at –60 °C. Pyrrole-β deuterium labelled **TMP-II** was used for ^{2}H NMR measurements. Concentration of **TMP-II**: ~2 mM for ^{2}H NMR and ~1 mM for EPR. Temperature: –60 °C for ^{2}H NMR and 3.7 K for EPR. Measurement conditions were unchanged during the experiments to compare the signal intensities. (a: red) **TMP-II**, (b: blue) after the addition of 2.5 equiv of AcOH (5.0 mM) to the solution (a), (c: black) after addition of TBAI (5.0 mM) to the solution (b).

The disproportionation of **TMP-II** was further confirmed by ^{2}H NMR and EPR spectroscopy. Figure 3 shows ^{2}H NMR spectra for the reaction of pyrrole-β deuterated **TMP-II** with AcOH at –60 °C. The pyrrole-β deuterium signal for **TMP-II** is observed at 6 ppm from TMS and this is consistent to the previous report.[7] When AcOH is added to the solution of **TMP-II**, new ^{2}H NMR signals are observed at 109 ppm and –11 ppm at the same intensities. These ^{2}H NMR shifts are close to those for acetate complexes of **TMP-III** and **TMP-I**, respectively.[13] The acetates formed after the protonation may work as the axial ligands of **TMP-I** and **TMP-III**. The signal intensities indicate the formation of **TMP-I** and **TMP-III** at about 1:1 ratio. With the addition of TBAI, the ^{2}H NMR signal for **TMP-I** disappeared and the intensity of the signal for **TMP-III** becomes twice, confirming the assignments. The disproportionation reaction was also studied by EPR spectroscopy. As expected from S = 1 state of **TMP-II**, no EPR signal is observed in the perpendicular mode except for a small

peak at g ~ 6 resulting from **TMP-III** formed by the decomposition of **TMP-II** in the preparation of EPR sample (less than 7 % from EPR signal intensity). When AcOH is added, new EPR signals are observed. EPR signals at g = 5.9 and 2.0 are identical to those of **TMP-III** and small signals at g = 4.4, 3.6, and 1.98 are identical to those of **TMP-I**.[13] Comparison of the signal intensities with authentic samples also supports the formation of these complexes at 1:1 ratio although the signal intensities are significantly different (Figure S4). When TBAI was further added to the EPR sample, the EPR signals resulting from **TMP-I** disappeared and the intensity of the EPR signals for **TMP-III** becomes twice. All of these NMR and EPR measurements support the disproportionation reaction of **TMP-II** to **TMP-I** and **TMP-III** with AcOH. While the disproportionation reaction of **TMP-II** has been proposed in many studies, this is the first spectroscopic evidence on the disproportionation reaction.

To study the function of AcOH, we examined the reactions with other acids. We added trifluoroacetic acid (TFA), hydrochloric acid (HCl in diethyl ether) and 2,6-lutidinium triflate ($LutH^+$), instead of AcOH. Similar absorption spectral changes are observed even when 2.0 equiv of TFA is added to **TMP-II** in dichloromethane at –60 °C (Figure S5). The disproportionation reaction is also confirmed by ^2H NMR and EPR spectroscopy (Figure S6). The total amount of TFA for completion of the disproportionation reaction is smaller than that (3.0 equiv) of AcOH. **TMP-II** also undergoes the disproportionation reaction with the addition of 2.0 equiv of HCl (Figure S7 and S8). The NMR shifts in Figure S6 and S8 suggest the coordination of trifluoroacetate and chloride as the axial ligands, respectively. The disproportionation reaction was also observed when more than 4 equiv of $LutH^+$ was added to **TMP-II** (Figure S10). These results suggest that an added acid works as a proton donor and, as an acid becomes weaker, more acid is required to disproportionate **TMP-II**.

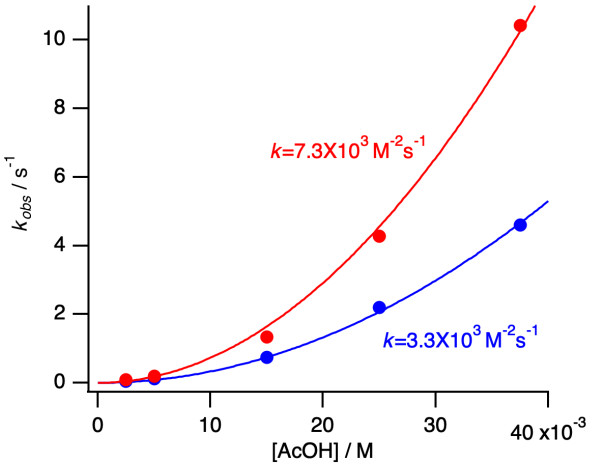

Figure 4. Dependence of the rate constant of the disproportionation reaction of **TMP-II** on the concentration of acetic acid in dichloromethane at –20 °C. Red circle: AcOH, blue circle: CD_3CO_2D. Red and blue lines are simulation curves with the second-order function, $k_{obs} = k[AcOH]^2$.

We performed stopped flow experiments to clarify the reaction mechanism. When **TMP-II** was rapidly mixed with AcOH in chlorobenzene at –20 °C, the absorption spectral change with clear isosbestic points was observed and a new intermediate could not be detected even in stopped flow time scale (Figure S11). The spectral change was very close to that of the second step of the titration experiment (Figure S1). These results indicate that the sequential protonation of **TMP-II** is the rate-limiting step. The time courses of the absorbance for the disproportionation reactions did not afford linear correlation on the plot of the inverse of the concentration of **TMP-II** over reaction time (1/[**TMP-II**]–t plot), but showed good linear correlation on the plot of logarithm of the concentration of **TMP-II** over reaction time (log[**TMP-II**]–t plot) (Figure S12). These results indicated that the disproportionation reaction is the first-order for the concentration of **TMP-II**. To evaluate the reaction-order for AcOH, we investigated the dependence of the rate constant on the concentration of AcOH (Figure S13 and Table S1). The rate constant increased with an increase in the concentration of AcOH and the dependence of the rate constant can be simulated well with a second-order function, $k_H = 7.3 \times 10^3\ M^{-2}s^{-1}$, (Figure 4). This indicates that two protons are involved in the disproportionation reaction.[14-15] When deuterium acetic acid (CD_3CO_2D, 99.5 %-D) was used, the rate constant for the disproportionation reaction becomes small, indicating involvement of the proton transfer process in the rate-limiting step, $k_D = 3.3 \times 10^3\ M^{-2}s^{-1}$. The estimated deuterium kinetic isotope effect ($k_H/k_D = 2.2$) was reasonable for the proton transfer process from AcOH.[16]

The results for the present kinetic study can be explained by the following reaction mechanism (Scheme 1). HX initially interacts with the oxo ligand of **II**, as recently reported by Karlin et al.[17] This step is an equilibrium process. Then, the second HX reacts with the singly-protonated **II** to afford a doubly protonated **II**, which immediately changes to an iron(III) porphyrin π-cation radical species having X as the axial ligand with releasing the oxo ligand as a water. This is a key step for the disproportionation reaction of **II**. Finally, the formed iron(III) porphyrin π-cation radical species works as an oxidant and reacts with another **II** to afford **I** and **III**. This

Scheme1.

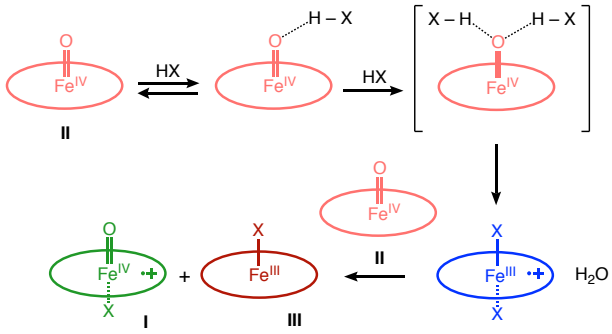

mechanism is supported by the present and previous studies.[17-25] The sequential addition of two protons to the oxo ligand of **II** is consistent to the titration experiment of AcOH (Figure S1). The binding of two protons has been reported for nonheme oxomanganese(IV) complexes.[18] The conversion between **II** and iron(III) porphyrin π-cation radical with acid and base has been reported in many studies.[7, 19-21] The exchange of the axial ligand to X is also reasonable because the aqua ligand has been known as a very weak axial ligand.[22-23] The oxidation of **II** to **I** with an iron(III) porphyrin π-cation radical has been reported by Balch et al.[24] and also supported by the redox potentials: $E_{1/2}(\mathbf{II}) < E_{1/2}(\mathbf{I})$.[25] In addition, the rate law based on this reaction mechanism predicts the first-order for the concentration of **II** and the second-order for the concentration of HX when the concentration of AcOH is low (see S.I.). This is also consistent to the present kinetic study.

Finally, we studied the effect of the disproportionation reaction of **II** on the oxidation of substrate. We examined the reaction of **TMP-II** with *p*-methoxystyrene and cyclooctene in the absence and presence of AcOH. **II** has been reported to be a less reactive compound than the corresponding **I**.[6-7] Therefore, the reactions of **TMP-II** with *p*-methoxystyrene and cyclooctenewere are very slow and afforded corresponding epoxides in 9 and 2 %, respectively. On the other hand, the reactions of **TMP-II** with *p*-methoxystyrene and cyclooctene in the presence of AcOH (2.0 equiv) produced corresponding epoxides in 24 % and 12 %, respectively. The reactions of authentic **TMP-I** afford the epoxides in 61 % and 39 % yields. These results indicate that the yields of the epoxides from the disproportionation reaction of **TMP-II** are higher than those from **TMP-II** and about half for those from **TMP-I**. These results clearly indicate that the disproportionation reaction of **II** increases the yield of the product by the formation of **I** and may be a significant reaction pathway when **II** is generated in the presence of an acid under catalytic conditions.

In conclusion, we show direct evidence on the disproportionation reaction of oxoiron(IV) porphyrin complex with absorption, ^{2}H NMR, and EPR spectroscopy. Kinetic study of the disproportionation reaction indicates the second-order for the concentration of proton and the first-order for the concentration of **II**. Based on these results, we propose the disproportionation mechanism, involving the sequential addition of two protons to the oxo ligand of **II**, followed by the oxidation of another **II** to afford **I** and **III**.

ASSOCIATED CONTENT

Supporting Information. The Supporting Information is available free of charge on the ACS Publications website. Experimental and computational details, Figures S1 – S13, Table S1, and derivation of reaction rate based on Scheme 1.

AUTHOR INFORMATION

Corresponding Author

fujii@cc.nara-wu.ac.jp

Funding Sources

No competing financial interests have been declared.

ACKNOWLEDGMENT

This work was supported by grants from JSPS (Grant 17H03032 and 19H04581) and CREST. The authors thank IMS for accommodation of NMR and EPR measurements.

REFERENCES

1. Huang, X.; Groves, J. T., Oxygen Activation and Radical Transformations in Heme Proteins and Metalloporphyrins. *Chem. Rev.* **2018,** *118*, 2491-2553.
2. Nam, W., High-Valent Iron(IV)–Oxo Complexes of Heme and Non-Heme Ligands in Oxygenation Reactions. *Acc. Chem. Res.* **2007,** *40*, 522-531.
3. Fujii, H., Electronic Structure and Reactivity of High-Valent Oxo Iron Porphyrins. *Coord. Chem. Rev.* **2002,** *226*, 51-60.
4. Fujii, H., Model Complexes of Heme Peroxidases. In *Heme Peroxidases*, Raven, E.; Dunford, B., Eds. The Royal Society of Chemistry: London, 2016; pp 183-217.
5. Rittle, J.; Green, M. T., Cytochrome P450 Compound I: Capture, Characterization, and C-H Bond Activation Kinetics. *Science* **2010,** *330*, 933-937.
6. Chin, D.-H.; La Mar, G. N.; Balch, A. L., Role of Ferryl (FeO^{2+}) Complexes in Oxygen Atom Transfer Reactions. Mechanism of Iron(II) Porphyrin Catalyzed Oxygenation of Triphenylphosphine. *J. Am. Chem. Soc.* **1980,** *102*, 5945-5947.
7. Groves, J. T.; Gross, Z.; Stern, M. K., Preparation and Reactivity of Oxoiron(IV) Porphyrins. *Inorg. Chem.* **1994,** *33*, 5065-5072.
8. Jeong, Y. J.; Kang, Y.; Han, A. R.; Lee, Y. M.; Kotani, H.; Fukuzumi, S.; Nam, W., Hydrogen Atom Abstraction and Hydride Transfer Reactions by Iron(IV)-Oxo Porphyrins. *Angew. Chem. Int. Ed.* **2008,** *47*, 7321-4.
9. Pan, Z.; Newcomb, M., Kinetics and Mechanism of Oxidation Reactions of Porphyrin−Iron(IV)−Oxo Intermediates. *Inorg. Chem.* **2007,** *46*, 6767-6774.
10. Pan, Z.; Newcomb, M., Acid-Catalyzed Disproportionation of Oxoiron(IV) Porphyrins to give Oxoiron(IV) Porphyrin Radical Cations. *Inorg. Chem. Commun.* **2011,** *14*, 968-970.
11. Groves, J. T.; Stern, M. K., Synthesis, Characterization, and Reactivity of Oxomanganese(IV) Porphyrin Complexes. *J. Am. Chem. Soc.* **1988,** *110*, 8628-8638.
12. Fukuzumi, S.; Fujioka, N.; Kotani, H.; Ohkubo, K.; Lee, Y. M.; Nam, W., Mechanistic Insights into Hydride-Transfer and Electron-Transfer Reactions by a Manganese(IV)-Oxo Porphyrin Complex. *J. Am. Chem. Soc.* **2009,** *131*, 17127-17134.
13. Takahashi, A.; Yamaki, D.; Ikemura, K.; Kurahashi, T.; Ogura, T.; Hada, M.; Fujii, H., Effect of the Axial Ligand on the Reactivity of the Oxoiron(IV) Porphyrin π-Cation Radical Complex: Higher Stabilization of the Product State relative to the Reactant State. *Inorg. Chem.* **2012,** *51*, 7296-305.
14. Park, J.; Lee, Y. M.; Nam, W.; Fukuzumi, S., Bronsted Acid-Promoted C-H Bond Cleavage via Electron Transfer from Toluene Derivatives to a Protonated Nonheme Iron(IV)-Oxo Complex with No Kinetic Isotope Effect. *J. Am. Chem. Soc.* **2013,** *135*, 5052-5061.
15. Park, J.; Morimoto, Y.; Lee, Y. M.; Nam, W.; Fukuzumi, S., Unified View of Oxidative C-H Bond Cleavage and Sulfoxidation by a Nonheme Iron(IV)-Oxo Complex via Lewis Acid-Promoted Electron Transfer. *Inorg. Chem.* **2014,** *53*, 3618-3628.
16. Kujime, M.; Fujii, H., Spectroscopic Characterization of Reaction Intermediates in a Model for Copper Nitrite Reductase. *Angew. Chem. Int. Ed.* **2006,** *45*, 1089-92.
17. Ehudin, M. A.; Gee, L. B.; Sabuncu, S.; Braun, A.; Moenne-Loccoz, P.; Hedman, B.; Hodgson, K. O.; Solomon, E. I.; Karlin, K. D., Tuning the Geometric and Electronic Structure of Synthetic High-Valent Heme Iron(IV)-Oxo Models in the Presence of a Lewis Acid and Various Axial Ligands. *J. Am. Chem. Soc.* **2019,** *141*, 5942-5960.

18. Chen, J.; Yoon, H.; Lee, Y. M.; Seo, M. S.; Sarangi, R.; Fukuzumi, S.; Nam, W., Tuning the Reactivity of Mononuclear Nonheme Manganese(IV)-Oxo Complexes by Triflic Acid. *Chem. Sci.* **2015,** *6*, 3624-3632.
19. Groves, J. T.; Gilbert, J. A., Electrochemical Generation of an Iron(IV) Porphyrin. *Inorg. Chem.* **1986,** *25*, 123-125.
20. Calderwood, T. S.; Lee, W. A.; Bruice, T. C., Spectral and Electrochemical Identification of Iron(IV)-Oxo Porphyrin and Iron(IV)-Oxo Porphyrin π-Cation Species. *J. Am. Chem. Soc.* **1985,** *107*, 8272-8273.
21. Boaz, N. C.; Bell, S. R.; Groves, J. T., Ferryl Protonation in Oxoiron(IV) Porphyrins and its Role in Oxygen Transfer. *J. Am. Chem. Soc.* **2015,** *137*, 2875-85.
22. Kastner, M. E.; Scheidt, W. R.; Mashiko, T.; Reed, C. A., Molecular Structure of Diaquo-α,β,γ,δ-Tetraphenylporphinatoiron(III) Perchlorate and Perchlorato-α,β,γ,δ-Tetraphenylporphinatoiron(III). Two New Structural Types for Iron(III) Porphyrins. *J. Am. Chem. Soc.* **1978,** *100*, 666-667.
23. Scheidt, W. R.; Reed, C. A., Spin-State/Stereochemical Relationships in Iron Porphyrins: Implications for the Hemoproteins. *Chem. Rev.* **1981,** *81*, 543-555.
24. Balch, A. L.; Latos-Grazynski, L.; Renner, M. W., Oxidation of Red Ferryl $[(Fe^{IV}O)^{2+}]$ Porphyrin Complexes to Green Ferryl $[(Fe^{IV}O)^{2+}]$ Porphyrin Radical Complexes. *J. Am. Chem. Soc.* **1985,** *107*, 2983-2985.
25. Takahashi, A.; Kurahashi, T.; Fujii, H., Redox Potentials of Oxoiron(IV) Porphyrin π-Cation Radical Complexes: Participation of Electron Transfer Process in Oxygenation Reactions. *Inorg. Chem.* **2011,** *50*, 6922-8.

Table of Content

Spectroscopic Evidence for Acid-Catalyzed Disproportionation Reaction of Oxoiron(IV) Porphyrin to Oxoiron(IV) Porphyrin π-Cation Radical and Iron(III) Porphyrin

Kana Nishikawa, Yuki Honda, and Hiroshi Fujii*